

# Prediction of expansion of electric arc furnace oxidizing slag mortar using MNLR and BPN

Wen-Ten Kuo\* and Chuen-UI Juang

Department of Civil Engineering, National Kaohsiung University of Applied Sciences, No. 415, Chien-Kung Rd., Sanmin District, Kaohsiung 80778, Taiwan, R.O.C.

(Received February 6, 2017, Revised March 29, 2017, Accepted March 30, 2017)

**Abstract.** The present study established prediction models based on multiple nonlinear regressions (MNLRs) and back-propagation neural networks (BPNs) for the expansion of cement mortar caused by oxidization slag that was used as a replacement of the aggregate. The data used for the models were obtained from actual laboratory tests on specimens that were produced with water/cement ratios of 0.485 or 1.5, within which 0%, 10%, 20%, 30%, 40%, or 50% of the cement had been replaced by oxidization slag from electric-arc furnaces; the samples underwent high-temperature curing at either 80°C or 100°C for 1-4 days. The varied mixing ratios, curing conditions, and water/cement ratios were all used as input parameters for the expansion prediction models, which were subsequently evaluated based on their performance levels. Models of both the MNLR and BPN groups exhibited  $R^2$  values greater than 0.8, indicating the effectiveness of both models. However, the BPN models were found to be the most accurate models.

**Keywords:** electric arc furnace oxidizing slag (EOS); back-propagation neural network (BPN); multiple linear regression (MLR)

## 1. Introduction

The worsening of global warming has compelled many countries to look for alternative recycled resources to alleviate environmental harm. Recycled material from industrial waste, particularly slag from steel production, has been found to be extremely useful in a wide range of fields (Lun 2008, Qasraei 2009, Han *et al.* 2002, Maslehuddin *et al.* 2003). Steel slag can be used to replace part of the cement as a binder, and can thus mitigate the secondary pollution caused by the production of cement. In recent decades, major developments in steel slag treatment and processing technologies have made it possible to substitute steel slag for natural aggregates in road construction (Alexandre *et al.* 1993, Shen *et al.* 2009a, b, 2010). Electric-arc furnace reductive slag is the reductive byproduct of smelting scrap steel in electric-arc furnace plants. According to Chen *et al.* (1999) and Tavakoli *et al.* (2014), reductive steel slag is ternary CaO(MgO)-Al<sub>2</sub>O<sub>3</sub>(Fe<sub>2</sub>O<sub>3</sub>)-SiO<sub>2</sub> composed mainly of calcium, magnesium, aluminum, iron, and silicon, with properties akin to those of silicate cement clinker and blast furnace steel slag. Wang *et al.* (Wang 2010, Wang *et al.* 2010, 2011, Mahmoud *et al.* 2012) pointed out that the hydrous oxides, such as CaO and MgO, in steel slag are the cause of its unstable volume, and that structures built with steel slag, and without correct regulation, would tend to show expansion or cracking (Huang *et al.* 2010, 2014, Hwang *et*

*al.* 2010). Therefore, adequate stabilization, quality control, processing, and testing measures must be taken before steel slag can safely be used in construction. Kuo *et al.* (Kuo *et al.* 2014a, b, 2015) discovered that the unstable steel slag would tend to cause expansion and failure after undergoing high temperature curing, the temperature of which determined the time until deterioration and the pattern of failure. Exposure to high temperatures (215.7°C) causes irreversible, monotonically increasing expansion in expansive cements within a relatively short time span (Wang *et al.* 2011).

The basic principle of regression analysis is the generalized least squares method, which is the minimization of the sum of the squares of errors. The most suitable formula for the linear correlation between one dependent variable and multiple independent variables can be obtained from estimations based on sample data, because all variables are interrelated one way or another. Can be based on the collection of the sample data to predict the forecast model, and then find the best formula. The curve fitting process in multiple nonlinear regression (MNLR) can find the result with the maximal multiple correlation coefficient and minimal relative error through logarithmic equations, linear equations, and exponential equations (Shi *et al.* 2010). It can effectively simulate the influence of high temperature curing on expansive steel slag, and facilitate easy and reliable expansion modeling with spreadsheet software such as Excel (Hagan 2004).

Many researchers have conducted numerical analyses on the mechanical behaviors of recycled material used in civil engineering; among them, Shi and Li (Shi *et al.* 2010) and Jin and Zhang (Jin *et al.* 2006) tested the substitution of recycled material for cement, and Silva *et al.* (Silva *et al.*

---

\*Corresponding author, Professor  
E-mail: [wtkuo@cc.kuas.edu.tw](mailto:wtkuo@cc.kuas.edu.tw)

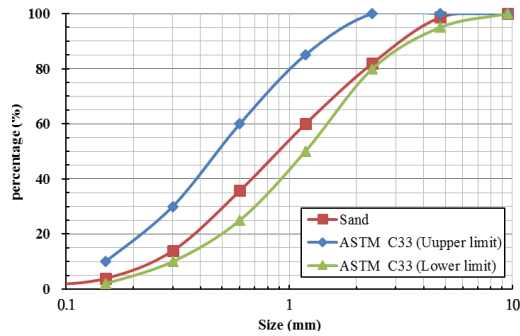


Fig. 1 The natural sand particle size distribution curve

2013, 2015) tested the shrinkage behaviors of recycled concrete. Their results indicated that shrinkage strain in concrete tends to grow with the amount of recycled material used to replace cement. In terms of compressive strength, Murat and Aimin (Murat *et al.* 2004) studied the compressive strength of concrete made with cinder and silica waste using an artificial neural network (ANN) test. That method was also adopted by Deshpande *et al.* (Tavakoli *et al.* 2014), Liu *et al.* (Deshpande *et al.* 2013), Khan *et al.* (Liu *et al.* 2011), Mohammed *et al.* (Khan *et al.* 2013), Tavakoli *et al.* (Mohammed *et al.* 2010), and Chithra *et al.* (Chithra *et al.* 2016). They all found the ANN approach to be satisfactory for prediction or estimation of compressive strength tests.

The literature surveyed did not make any mention of mathematical model for predicting cement mortar expansion induced by steel slag, and until now, researchers have only predicted compressive strength and drying shrinkage (Shi *et al.* 2010, Jin *et al.* 2006, Silva *et al.* 2013, 2015, Murat *et al.* 2004, Deshpande *et al.* 2013, Liu *et al.* 2011, Khan *et al.* 2013, Mohammed *et al.* 2010, Wang *et al.* 2014a, b, Kar *et al.* 2016). In this regard, the present study considered it plausible to find a solution through numerical analysis. A mathematical model was derived from laboratory results and the curve fitting function of Excel-2013. Will result in expansion of steel ballast factor are: free calcium oxide, magnesium oxide hydration reaction, curing time, and conservation of the environment (Beshears and Tutumluer 2013). Therefore, this study is based on the literature review of the expansion of the impact factors were including water/cement ratios (W/C), curing temperatures (CT), curing days (CD), and substitutions (S) were used with linear, logarithmic, and exponential models. The result with a determination coefficient ( $R^2$ ) closest to 1, with minimal root mean squared error (RMSE), and with minimal mean absolute percentage error (MAPE) was selected. Atici *et al.* (2011) found that a comparable approach enabled effective simulation of the expansion in cement mortar induced by steel slag (Atici *et al.* 2011, Shu *et al.* 2016).

Another approach is the use of an ANN, which is a useful mathematical prediction tool inspired by biological neural networks (Tavakoli *et al.* 2014). An ANN is capable of processing data rapidly without the need for typical testing mechanisms or assumptions (Wang *et al.* 2015, Sakthivel Ravichandran *et al.* 2016), because the neurons are interconnected; even when the input parameters are

Table 1 Physical and chemical properties of the Electric arc Furnace Oxidizing Slag

Oxides		(%)								
Al <sub>2</sub> O <sub>3</sub>		4.82								
SiO <sub>2</sub>		45.99								
Fe <sub>2</sub> O <sub>3</sub>		0.59								
CaO		40.40								
Chemical characteristics (%)	MgO	3.16								
	K <sub>2</sub> O	0.04								
	SO <sub>3</sub>	0.48								
	Na <sub>2</sub> O	0.12								
	TiO <sub>2</sub>	1.69								
	f- CaO	1.00-1.20								
	Aggregate size (mm)		Coarse aggregate	Fine aggregate						
	Physical characteristics		19-12.5	12.5-9.5	9.5-4.75	4.75-2.36	2.36-1.18	1.18-0.6	0.6-0.3	0.3-0.15
		Specific gravity (SSD)	2.91	2.95	2.97	3.08	3.07	3.04	2.99	2.93
		Absorption (%)	1.2	1.5	1.6	1.7	1.8	2.9	3.4	4.1

nonlinearly correlated with the output parameters, solutions can be obtained through functional approximation and curve fitting (Aggarwal *et al.* 2013). Theoretically, the high accuracy of ANNs in prediction can be attributed to the fact that they can be trained repeatedly to approximate errors to a level suitable for an accurate prediction (Aggarwal *et al.* 2013, Luo *et al.* 2005, Naik *et al.* 2013). The present study used the back-propagation neural network (BPN) of Matlab-2013, which is a gradient descent method derived from extending the Widrow-Hoff learning rule to a multilayer nonlinear differential transfer function network. From the perspective of curve fitting, the function approximation (nonlinear regression) of BPN is effective for the interpolation of data, but it is not necessarily accurate in extrapolation.

## 2. Material properties

### 2.1 Cement

This study used Type I Portland cement from Taiwan Cement Co. Ltd, which conformed to the ASTM C150 I standard specification for Portland cement.

### 2.2 Sand

The natural river sand was from Ligang River in Pingtung County, Taiwan. The sand had a fineness modulus of 3.06, apparent specific gravity of 2.74, saturated-surface-dry of 2.63, and water absorption by mass of 2.4%. Its particle size distribution is as shown in Fig. 1.

### 2.3 Electric arc furnace oxidizing slag

The electric-arc furnace oxidization slag (EOS) that oxidization slag that was used as a replacement of the aggregate was from a stainless steel plant of the China Steel

Table 2 Mix proportions

	Item	Cement	Water	Sand	EOS
Ratio prediction model experiment	NRef.	541	262	1488	-
	CRef.	200	300	1674	-
	NEOS 10	545	264	1349	150
	NEOS 20	549	266	1208	302
	NEOS 30	553	268	1064	456
	NEOS 40	557	270	919	613
	NEOS 50	545	264	749	749
	CEOS 10	202	302	1519	169
	CEOS 20	203	305	1361	340
	CEOS 30	205	307	1201	515
CEOS 40	207	310	1038	692	
CEOS 50	208	313	872	872	
Verification experimental model ratio	Item	Cement	Water	Sand	EOS
	EOS10	541	264	1349	150
	EOS15	545	265	1279	226
	EOS30	553	268	1064	456
	EOS35	555	269	934	535
EOS65	567	275	557	1006	

Corporation. The batch was sifted with a #4 sieve to eliminate coarse grains. The physical and chemical composition of the sand is as shown in Table 1.

### 3. Data collection

Table 2 shows specimens of cement mortar bars with varied EOS substitution (S) percentages (S=10%, 20%, 30%, 40%, and 50%) and W/C ratios (W/C=0.485 & 1.5). The specimens were subjected to curing temperatures (CTs) of 80°C and 100°C for 1-4 curing days (CDs). Non-dimensional (Neela Deshpande *et al.* 2014) input parameters include W/C, CT, Mandatory input parameters called as raw data including EOS replacement for all cement mortar constants. The target parameter is Expansion, and the output value is also Expansion.

#### 3.1 Testing method

Three cement mortar specimens were made for each of the aforementioned combinations of S, W/C, and curing, and they were wiped dry before being measured. The extent of expansion was determined by the maximum growth in length on the four sides of an individual 300 mm specimen. The calculation of expansion is expressed in Eq. (1)

$$Expansion\ expressed = \frac{L_0 - L_1}{L_0} \times 100\% \quad (1)$$

Where the specimen's original length upon leaving the mold is denoted as L<sub>0</sub>, and L<sub>1</sub> denotes the expanded length.

#### 3.2 Verification data

Table 3 The basic model variables

Model ID	Dependent variables	Number of samples	MNL	BPN
M1	S, CD	48	MNL1	BPN1
M2	S, CD, CT	96	MNL2	BPN2
M3	S, CD, CT, W/C	192	MNL3	BPN3

Table 4 Prediction equation and the coefficient of determination for MNL1

W/C	Curing temperature (°C)	Equations	Coefficient determination (R <sup>2</sup> )
0.485	80	$y_{LI} = 0.0015S + 0.0124CD + 0.0063$	0.88
		$y_{EX} = 0.0261e^{((0.0214S)(0.1868CD))}$	0.90
		$y_{LO} = 0.0809 \log(S) + 0.0619 \log(CD) - 0.0550$	0.80
	100	$y_{LI} = 0.0013S + 0.0085CD + 0.0339$	0.70
		$y_{EX} = 0.0369e^{((0.0201S)(0.1385CD))}$	0.78
		$y_{LO} = 0.0779 \log(S) + 0.0547 \log(CD) - 0.0358$	0.75
1.5	80	$y_{LI} = 0.0020S + 0.00067CD + 0.0139$	0.83
		$y_{EX} = 0.0211e^{((0.0343S)(0.1717CD))}$	0.89
		$y_{LO} = 0.1248 \log(S) + 0.0457 \log(CD) - 0.1015$	0.80
	100	$y_{LI} = 0.0024S + 0.0080CD + 0.0283$	0.82
		$y_{EX} = 0.0387e^{((0.0270S)(0.1520CD))}$	0.81
		$y_{LO} = 0.0916 \log(S) + 0.0616 \log(CD) - 0.0392$	0.88

Note: The code in the equation, LI for the multiple linear equations, EX as multiple exponential equation, LO for the multiple logarithmic equation

The setting of a prediction model should comply with the practice of actual factories; therefore, a new batch of EOS that had not been stabilized was collected to verify the model through S and CD values modified by interpolation and extrapolation. The verified variables are shown in Table 2.

#### 3.3 The test equipment for expansion of cement mortar

The EOS cement mortar expansion experiment was carried out in this study. The length of the cement mortar was measured by the electronic length comparison analyzer, and the length of the cement mortar was measured.

### 4. Methodology

In the present study, three different models were used with established MNL and BPN methods. For each model, input and output parameters were modified, as shown in Table 3.

#### 4.1 Multivariate nonlinear regression analysis and correlation coefficient

Excel's numerical analysis was used for the regression analysis. According to Atici (Atici *et al.* 2011), the validity of a prediction model depends on the determination

Table 5 Prediction equation and the coefficient of determination for MNLR2

W/C	Equations	Coefficient of determination (R <sup>2</sup> )
0.485	$y_{LI} = 0.0014S + 0.0107CD + 0.0008CT - 0.0503$	0.82
	$y_{EX} = 0.0119e^{((0.0210S)(0.1668CD)(0.0105CT))}$	0.87
	$y_{LO} = 0.0798 \log(S) + 0.0589 \log(CD) + 0.1349 \log(CT) - 0.3093$	0.78
1.5	$y_{LI} = 0.0021S + 0.0072CD + 0.0011CT - 0.0738$	0.83
	$y_{EX} = 0.0038e^{((0.0332S)(0.1671CD)(0.0220CT))}$	0.88
	$y_{LO} = 0.1174 \log(S) + 0.0529 \log(CD) + 0.2726 \log(CT) - 0.6123$	0.79

Table 6 Prediction equation and the coefficient of determination for MNLR3

Equations	Coefficient of determination (R <sup>2</sup> )
$y_{LI} = 0.0017S + 0.0088CD + 0.0009CT + 0.0056W/C - 0.0613$	0.78
$y_{EX} = 0.0073e^{((0.0250S)(0.1600CD)(0.0144CT)(0.0197W/C))}$	0.82
$y_{LO} = 0.0933 \log(S) + 0.0543 \log(CD) + 0.1822 \log(CT) + 0.0226 \log(W/C) - 0.4109$	0.75

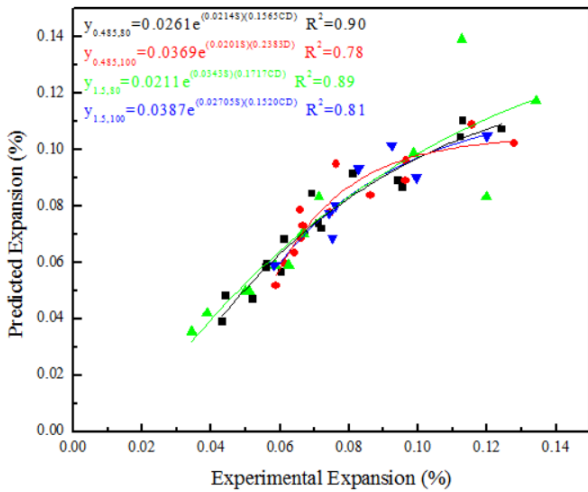


Fig. 2 Predicted Expansion vs Experimental Expansion for model MNLR1 to Exponential equation

coefficient (R<sup>2</sup>), which is calculated as Eq. (2)

$$R^2 = 1 - \frac{\text{Sum of squares of residuals}}{\text{Sum of squares of predicted values}} \quad (2)$$

The closer the determination coefficient is to 1, the better the prediction results are. Tables 4, 5, and 6 list the various prediction results of MNLR1, MNLR2, and MNLR3, respectively.

They all indicated that exponential equations had the most favorable results because the determination coefficients were greater than 0.6. The accuracy of expansion prediction was illustrated by comparing observed test results with the results of exponential equations through multiple nonlinear regression, as shown in Figs. 2, 3, and 4. Fig. 2 displays the prediction results of MNLR1, in which the a in ya,b denotes W/C, and the b denotes CT. Fig. 2 clearly shows that the test results and prediction results had a highly linear relationship, indicating a highly favorable level of prediction accuracy. Fig. 3 is the exponential model of MNLR2, which reveals that when the CTs were treated as non-dimensional input parameters and were used as the

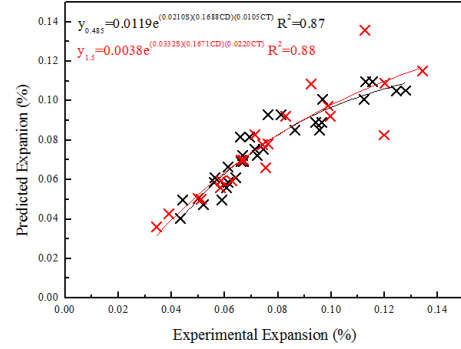


Fig. 3 Predicted Expansion vs Experimental Expansion for model MNLR2 to Exponential Equation

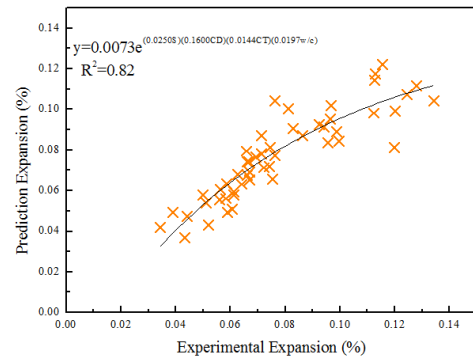


Fig. 4 Predicted Expansion vs Experimental Expansion for model MNLR3 to Exponential equation

third variable, prediction accuracy was markedly improved and the model conformed more accurately to observed data. Fig. 4 displays the prediction results of MNLR3, which reveal that although curve fitting exponential equations were feasible for conducting multiple variable prediction simulation of cement mortar expansion, absolute coefficients alone were inadequate for the verification of prediction accuracy.

MAPE can be calculated as Eq. (3), and a value less than 10 signifies high prediction accuracy (Lewis *et al.* 1982, Jordi *et al.* 2011). The MAPE values in the regression model were 8.0858, 8.7030, 9.3428, and 8.1184 for MNLR1, 8.7337 and 9.2896 for MNLR2, and 10.8053 for MNLR3, respectively.

$$\left( \frac{1}{n} \sum_{i=1}^n \left| \frac{\text{Observations expansion value} - \text{Predictions expansion value}}{\text{Observations expansion value}} \right| \right) \times 100\% \quad (3)$$

RMSE can be calculated as Eq. (4), where n denotes the number of observations. The closer the RMSE value is to 0, the more accurate the curve fitting result is (Iker *et al.* 2008).

$$\sqrt{\frac{1}{n} \sum_{i=1}^n (\text{Observations expansion value} - \text{Predictions expansion value})^2} \quad (4)$$

The RMSE values were 0.0075, 0.0103, 0.0139, and 0.0085 for MNLR1, 0.0089 and 0.0122 for MNLR2, and 0.0115 for MNLR3. The fact that all of these values were less than 0.01 signifies high levels of reliability. The results of the exponential simulation model with multiple nonlinear regression for EOS cement mortar are shown in Table 7.

Table 7 Results of Multiple non-linear regression

Model	Dependent variables	coefficient of determination (R <sup>2</sup> )	Statistics parameters	
			MAPE	RMSE (%)
MNLR1	W/C=0.485, CT=80	0.90	8.0858	0.0075
	W/C=0.485, CT=100	0.78	8.7030	0.0103
	W/C=1.5, CT=80	0.89	9.3428	0.0139
	W/C=1.5, CT=100	0.81	8.1184	0.0085
MNLR2	W/C=0.485	0.87	8.7337	0.0089
	W/C=1.5	0.88	9.2896	0.0122
MNLR3	--	0.82	10.8053	0.0115

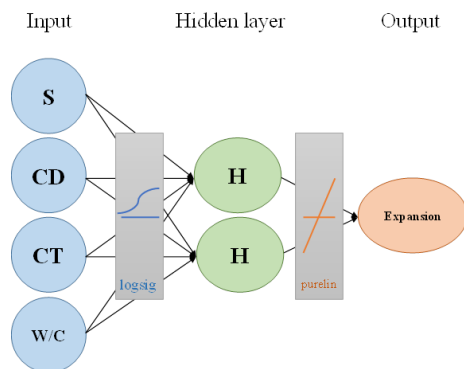


Fig. 5 Back-propagation neural network Topology

#### 4.2 EOS's back-propagation neural network

Numerous algorithms have been developed for ANN models (Gulbandilar and Kocak 2016). Some noteworthy learning rules are Coincidence Learning: Hebb's law, ADALINE, Performance Learning: ADALINE, Competitive Learning: Kohonen's law, Filter Learning: Grossberg's law, and Spatiotemporal Learning: Kosko and Klopf's law. In terms of topologies, feed forward networks (such as backpropagation networks and radial basis function networks) can be distinguished from recurrent networks (such as the Hopfield network). Kisi (Ozgun Kisi *et al.* 2007) predicted river flow rate with the conjugate-gradient algorithm, back propagation algorithm, cascade algorithm, and Levenberg-Marquardt algorithm and found that the prediction models of the cascade algorithm and Levenberg-Marquardt algorithm were the closest to the observed data. The Levenberg-Marquardt algorithm is a feed-forward network that is most widely used in ANN prediction modeling, and back-propagation is a method that calculates gradients in multilayer nonlinear networks. The present study used a BPN, of which the topological structures are shown in Fig. 5.

The study used the BPN toolbox developed by Matlab for three ANN models, namely BPN1, BPN2, and BPN3. Then, 70% of the data were assigned to the training set, 15% to the validation set, and 15% to the testing set. The basic parameters were as follows:

- (a) The hidden layer contained 2 neurons.
- (b) Training was repeated 10000 times.
- (c) The minimum error was allowed to converge to 0.00001.

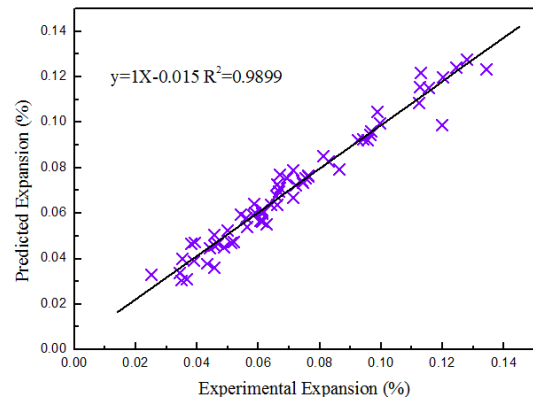


Fig. 6 Predicted Expansion vs Experimental Expansion for model BPN1

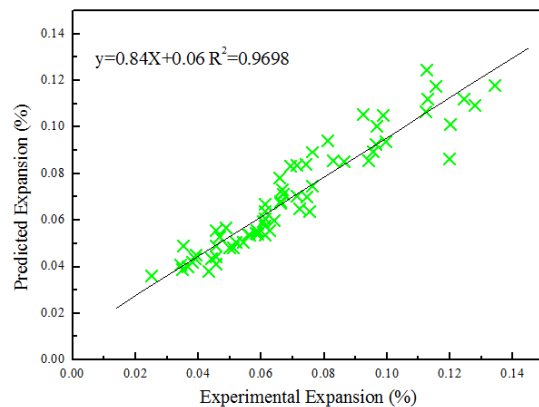


Fig. 7 Predicted Expansion vs Experimental Expansion for model BPN2

- (d) The learning rate was 0.1.
- (e) The momentum factor was 0.5.
- (f) The relationship between the input and hidden layers was a log-sigmoid transfer function (logsig).
- (g) The relationship between the hidden and output layers was a linear transfer function (purelin).

Because the functional assumptions of the BPN were logsig and purelin, the output values were constrained to be between 0 and 1. Therefore, to ensure the study's accuracy, the BPN prediction data had to be normalized in advance, to convert the observed data to the range from 0 to 1. The normalization equation was as follows Eq. (5)

$$X_{new} = \frac{X_{original} - X_{min}}{X_{max} - X_{min}} \quad (5)$$

The training of a BPN is intended to minimize error by iterative convergence. Table 7 lists the absolute coefficients for the training, validation, and testing of each model and the whole data pool. All of the absolute coefficient values were greater than 0.9 and some of them were approximately equal to 1, which indicated that the results from the BPN model accurately conformed to the observed test data. Furthermore, whereas MNLR2 had an absolute coefficient of only 0.82, BPN3 had an absolute coefficient of 0.96, which implies that BPN3 was capable of a more accurate prediction than that of MNLR2. The BPN prediction values and observed test values are shown in Figs. 6, 7, and 8.

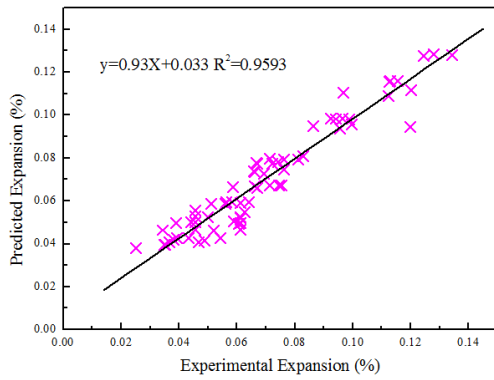


Fig. 8 Predicted Expansion vs Experimental Expansion for model BPN3

Table 8 Coefficient determination for back-propagation neural network models

Model	Coefficient determination ( $R^2$ )			
	Training	Testing	Validation	Overall data
BPN1	0.9987	0.9973	0.9956	0.9975
BPN2	0.9881	0.9889	0.9876	0.9872
BPN3	0.9699	0.9770	0.9695	0.9683

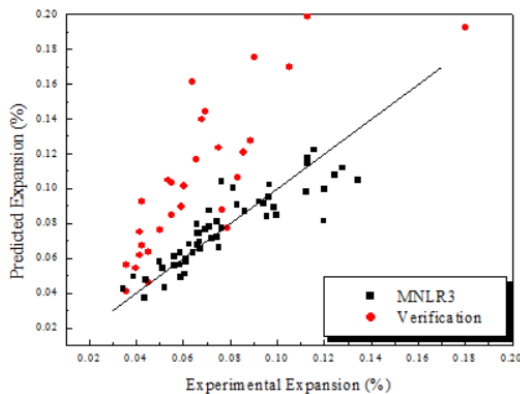


Fig. 9 Predicted Expansion vs Experimental Expansion for model MNLRV

Table 8 displays the determination coefficients of the BPN models. The MAPE values for the three models were 5.7799, 9.4302, and 9.8982, respectively; and the RMSE values were 0.00254, 0.00864, and 0.00741, respectively. These particularly low values indicate a particularly low difference between the observed data and predicted data, representing a highly favorable prediction accuracy (Kong *et al.* 2016).

#### 4.3 Prediction model validation

The present study conducted two types of validation for the Multiple non-linear regression verification (MNLRV) and Back-propagation neural network verification (BPNV). Fig. 9 displays the results of the MNLRV, which was based on the model of MNLR3, and verified with observed test values taken from specimens with varied curing times. The comparison reveals that although a large difference existed between the model and verification values, you can know

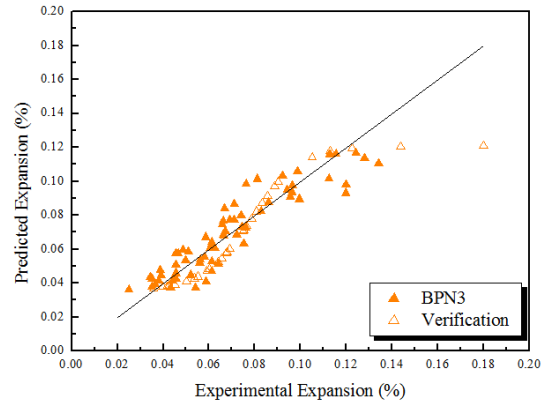


Fig. 10 Predicted Expansion vs Experimental Expansion for model BPNV

that the current factories are to pay attention to the problem of steel slag expansion, and to be first to stabilize the operation, the verification results were all above those of the model, which indicated a safety range of approximately 1.14-2.34 for the prediction model.

Fig. 10 displays the BPNV results, which were based on the model of BPN3. Although the model exhibited an  $R^2$  value of almost 1, which signified a particularly high prediction accuracy, the application of the BPN model to other models would be inadequate because the BPN model was established on specific variables.

### 5. Conclusions

- The MNLRV results show that the exponential curve equation predicts that the steel slag expansion model is closer to the actual result.
- BPNs can be used to predict the expansion of EOS for cement mortar more effectively than MNLR.
- MNLR and BPNs have the same results, with the exponential model of MNLR2 matched the prediction results of BPN2, and both exhibited the most favorable  $R^2$ , MAPE, and RMSE values.
- From the verification results that the forecast model of the security range of 1.14-2.34, can be used as a reference for future projects.
- MNLR and BPN have effectively established EOS induced expansion prediction model of cement mortar.

### Acknowledgements

The authors would like to thank the Ministry of Science and Technology of Taiwan for their financial support of this research under Contract No. MOST 104-2221-E-151-040.

### References

Aggarwal, P., Aggarwal, Y., Siddique, R., Gupta, S. and Garg, H. (2013), "Fuzzy logic modeling of compressive strength of high-strength concrete (HSC) with supplementary cementitious material", *J. Sustain. Cement Base. Mater.*, **2**(2), 1-16.

- Alexandre, J. and Boudonnet, J.Y. (1993), "Les laitiers d'aciérie LD et leurs utilisations routières", *Laitiers Sidérurgiques*, **75**, 57-62.
- Atici, U. (2011), "Prediction of the strength of mineral admixture concrete using multivariable regression analysis and an artificial neural network", *Exp. Syst. Appl.*, **38**(8), 9609-9618.
- Beshars and Tutumlu. (2013), *Reclaimed Asphalt Pavement with Steel Slag Aggregate*, TR NEWS 288, 46-47, September-October.
- Chithra, S., Senthil Kumar, S.R.R., Chinnaraju, K. and Alfin Ashmita, F. (2016), "A comparative study on the compressive strength prediction models for high performance concrete containing nano silica and copper slag using regression analysis and artificial neural networks", *Constr. Build. Mater.*, **114**, 528-535.
- Deshpande, N., Londhe, S. and Kulkarni, S. (2014), "Modeling compressive strength of recycled aggregate concrete by artificial neural network", model tree and non-linear regression, *J. Sustain. Built Environ.*, **3**(2), 187-198.
- Deshpande, N., Londhe, S. and Kulkarni, S.S. (2013), "Modelling compressive strength of recycled aggregate concrete using neural networks and regression", *Concrete Res. Lett.*, **4**(2), 580-590.
- Gulbandilar, E. and Kocak, Y. (2016), "Application of expert systems in prediction of flexural strength of cement mortars", *Comput. Concrete*, **18**(1), 1-16.
- Hagan, D.I. (2004), *Neural Network Design*, Thomson.
- Han, Y.M., Jung, H.Y., Seong, S.K. (2002), "A fundamental study on the steel slag aggregate concrete", *Geosyst. Eng.*, **5**(2), 38-45.
- Huang, K.J., Deng, M., Shen, Y.Q. and Mo, L.W. (2010), "Failure analysis of early age cracking of paving concrete in donghai country", *J. Wuhan Univ. Tech-Mater. Sci. Ed.*, **32**(5), 62-66.
- Huang, Q. (2014), "Add prediction mode of waste LCD glass concrete elaboration mechanics and engineering", Ph.D. Dissertation, National Kaohsiung Institute of Technology in Civil Engineering and Disaster Prevention University of Applied Sciences, Taiwan.
- Hwang, C.L. (2010), *High Performance Concrete Theory and Practice*, Taipei, Zhan Shi, Taiwan.
- Ilker, B.T. and Mustafa, S. (2008), "Prediction of compressive strength of concrete containing fly ash using artificial neural networks and fuzzy logic", *Comput. Mater. Sci.*, **41**(3), 305-311.
- Jin, Z.H. and Zhang, L. (2006), *Accelerated Test Method by Binary Regression for Cement Strength*, Testing Centre of Sinohydro Engineering Bureau 15 Co. Ltd, Shannxi, China.
- Jordi, M. (2011), "Mean absolute percentage error and bias in economic forecasting", *Eco. Lett.*, **113**(3), 259-262.
- Kar, A., Ray, I., Unnikrishnan, A. and Halabe, U.B. (2016), "Prediction models for compressive strength of concrete with alkali-activated binders", *Comput. Concrete*, **17**(4), 523-539.
- Khan, S.U., Ayub, T. and Rafeeqi, S.F.A. (2013), "Prediction of compressive strength of plain concrete confined with ferrocement using artificial neural network (ANN) and comparison with existing mathematical models", *Am. J. Civil Eng. Arch.*, **1**(1), 7-14.
- Kisi, O. (2007), "Streamflow forecasting using different artificial neural network algorithms", *J. Hydrol. Eng.*, **12**(5), 532-539.
- Kong, L., Chen, X. and Du, Y. (2016), "Evaluation of the effect of aggregate on concrete permeability using grey correlation analysis and ANN", *Comput. Concrete*, **17**(5), 613-628.
- Kuo, W.T. and Shu, C.Y. (2014), "Application of high-temperature rapid catalytic technology to forecast the volumetric stability behavior of containing steel slag mixtures", *Constr. Build. Mater.*, **50**, 463-470.
- Kuo, W.T. and Shu, C.Y. (2015), "Expansion behavior of low-strength steel slag mortar during high-temperature catalysis", *Comput. Concrete*, **16**(2), 261-274.
- Kuo, W.T., Shu, C.Y. and Han, Y.W. (2014), "Electric arc furnace oxidizing slag mortar with volume stability for rapid detection", *Constr. Build. Mater.*, **53**, 635-641.
- Lewis, C.D. (1982), *Industrial and Business Forecasting Method*, Butterworth Scientific Publishers, London, U.K.
- Liu, J., Li, H. and He, C. (2011), "Predicting the compressive strength of concrete using rebound method and artificial neural network", *ICIC Expr. Lett.*, **5**(4), 1115-1120.
- Lun, Y., Zhou, M., Cai, X. and Xu, F. (2008), "Methods for improving volume stability of steel slag as fine aggregate", *J. Wuhan Univ. Tech-Mater. Sci. Ed.*, **23**(5), 737-742.
- Luo, Y.H., Han, Y.F. and Gao, Z.G. (2005), "Curve-fitting of concrete's rebound strength testing based on the neural network", *Res. Appl. Build. Mater.*, **3**, 7-9.
- Mahmoud, A. (2012), "Laboratory studies to investigate the properties of concrete mixes containing steel slag as a substitute for virgin aggregates", *Constr. Build. Mater.*, **26**(1), 475-480.
- Mashrei, M.A., Abdulrazzaq, N., Abdalla, T.Y. and Rahman, M.S. (2010), "Neural networks model and adaptive neuro-fuzzy inference system for predicting the moment capacity of ferrocement members", *Eng. Str.*, **32**(6), 1723-1734.
- Maslehuddin, M., Sharif, A.M., Shameem, M., Ibrahim, M. and Barry, M.S. (2003), "Comparison of properties of steel slag and crushed limestone aggregate concretes", *Constr. Build. Mater.*, **17**(2), 105-112.
- Mohammed, A., Mashrei, N.A. and Turki, Y. (2010), "Neural networks model and adaptive neuro-fuzzy inference system for predicting the moment capacity of ferrocement members", *Eng. Struct.*, **32**(6), 1723-1734.
- Murat, P. and Aimin, X. (2004), "Value-added utilisation of waste glass in concrete", *Cement Concrete Res.*, **34**(1), 81-89.
- Naik, U. and Kute, S. (2013), "Span-to-depth ratio effect on shear strength of steel fiber reinforced high-strength concrete deep beams using ANN method", *J. Adv. Struct. Eng.*, 1-12.
- Qasrawi, H. (2009), "Use of low CaO unprocessed steel slag in concrete as fine aggregate", *Constr. Build. Mater.*, **23**(2), 1118-1125.
- Sakthivel, P.B., Alagumurthi, A. and Modeling, N. (2016), "Modeling and prediction of flexural strength of hybrid mesh and fiber reinforced cement-based composites using artificial neural network (ANN)", *J. Geomater.*, **10**(1), 1623-1635.
- Shen, D.H., Wu, C.M. and Du, J.C. (2009), "Laboratory investigation of basic oxygen furnace slag for substitution of aggregate in porous asphalt mixture", *Constr. Build. Mater.*, **23**(1), 453-461.
- Shen, W., Zhou, M. and Ma, W. (2009), "Investigation on the application steel slag-fly ash-phosphogypsum solidified material as road base material", *Hazard. Mater.*, **164**(1), 99-104.
- Shi, J.P. and Li, X. (2010), "Build 28d compressive strength forecasting equation by curve fitting", *Cement Eng.*, **4**, 77-78.
- Shu, C.Y., Kuo, W.T. and Juang, C.U. (2016), "Analytical model of expansion for electric arc furnace oxidizing slag-containing concrete", *Comput. Concrete*, **18**(5), 937-950.
- Silva, R.V., Brito, J. and Dhir, R.K. (2013), "Prediction of compressive strength of recycled aggregate concrete using artificial neural networks", *Constr. Build. Mater.*, **40**, 1200-1206.
- Silva, R.V., Brito, J. and Dhir, R.K. (2015), "Prediction of the shrinkage behavior of recycled aggregate concrete: A review", *Constr. Build. Mater.*, **77**, 327-339.
- Tavakoli, H.R., Lotfi, O.O., Falahtabar, S.M. and Soleimani, S.S. (2014), "Prediction of combined effects of fibers and nano-silica on the mechanical properties of self-compacting concrete using artificial neural network", *Lat. Am. J. Sol. Str.*, **11**(11),

- 1906-1923.
- US Federal Environment Protection Agency (2010), *Use of Recycled Industrial Materials in Roadways*.
- Wang, B.X., Man, T.N. and Jin, H.N. (2015), "Prediction of expansion behavior of self-stressing concrete by artificial neural networks and fuzzy inference systems", *Constr. Build. Mater.*, **84**, 184-191.
- Wang, C.C., Chen T.T., Wang, H.Y. and Huang, C. (2014), "A predictive model for compressive strength of waste LCD glass concrete by nonlinear-multivariate regression", *Comput. Concrete*, **13**(4), 531-545.
- Wang, C.C., Wang, H.Y. and Huang, C. (2014), "Predictive models of hardened mechanical properties of waste LCD glass concrete", *Comput. Concrete*, **14**(5), 577-597.
- Wang, G. (2010), "Determination of the expansion force of coarse steel slag aggregate", *Constr. Build. Mater.*, **24**(10), 1961-1966.
- Wang, G., Wang, Y. and Gao, Z. (2010), "Use of steel slag as a granular material: Volume expansion prediction and usability criteria", *J. Hazard. Mater.*, **184**(1), 555-560.
- Wang, W.C., Liu, C.C., Lee, C. and Yu, S.K. (2011), "Preliminary research of expansion problem and treated method of using slag as aggregate of concrete", *Proceedings of the TCI Conference on Concrete Engineering*.